solar

MDPI

Article

Enhancing Industrial Buildings' Performance through Informed Decision Making: A Generative Design for Building-Integrated Photovoltaic and Shading System Optimization

Neri Banti *, Cecilia Ciacci *, Frida Bazzocchi and Vincenzo Di Naso

Department of Civil and Environmental Engineering, University of Florence, 50139 Florence, Italy; frida.bazzocchi@unifi.it (F.B.); vincenzo.dinaso@unifi.it (V.D.N.)
* Correspondence: neri.banti@unifi.it (N.B.); cecilia.ciacci@unifi.it (C.C.)

Abstract: The Italian industrial sector contains 22% of the final energy demand due to the poor energy performance of manufacturing buildings. This proposed study aimed to evaluate retrofit interventions for existing industrial buildings integrating photovoltaic solutions into the external envelope to improve both the environmental sustainability and the facade performance. The methodology is based on an innovative procedure including BIM and generative design tools. Starting from the Revit model of a representative case study, interoperability with energy analysis plugins via Grasshopper were exploited to optimize the differently oriented facade layout of photovoltaic modules to maximize the electricity production. In the case of comparable facade sizes, the building orientation had a minor impact on the results, although a southern exposure was preferable. The optimized configuration involved the installation of PV panels with a tilt angle ranging from −35° to −75°. The best compromise solution between the panel surface area and energy production during the summer solstice involves 466 m^2 of PV modules. The design-optioneering approach was used to define possible alternatives to be explored for the possible installation of solar shading systems on existing windows. In this case, the impact on visual comfort within the working environment was chosen as a reference parameter, along with the value of the indoor air temperature. A decrease in this parameter equal to 0.46 was registered for the solution with horizontal (or nearly horizontal) shaders and a spacing ranging between 0.2 and 0.4. The integration of the BIM environment with generative design tools effectively assists decision-making processes for the selection of technological solutions in the building sector.

Keywords: BIPV; BIM; optimization; industrial buildings; Grasshopper

Citation: Banti, N.; Ciacci, C.; Bazzocchi, F.; Di Naso, V. Enhancing Industrial Buildings' Performance through Informed Decision Making: A Generative Design for Building-Integrated Photovoltaic and Shading System Optimization. *Solar* **2024**, *4*, 401–421. https://doi.org/10.3390/solar4030018

Academic Editors: Juan B. Carda Castelló and Javier Muñoz Antón

Received: 5 June 2024
Revised: 9 July 2024
Accepted: 17 July 2024
Published: 25 July 2024

1. Introduction

According to the Global Status Report, the building and industrial sectors can be considered two of the most energy-intensive ones, accounting for 30% and 33% of the total global energy consumption, respectively [1]. Moreover, the former covers up to 37% of CO_2 emissions considering residential and non-residential intended uses and the related construction industries [2]. For this reason, the European Commission has recently set the goal of a nearly zero-emissions level for new buildings by 2030 through a new directive to keep up with the ambitious European goals to achieve a carbon-free economy by 2050 [3]. At the same time, the Observatory of the European Building Stock points out that 80% of the existing building heritage will still be in use by 2050 [4], and renovation initiatives for at least 43% of the existing buildings are expected in the future. Considering the different intended uses of existing facilities, industrial and manufacturing facilities have been generally ignored by both institutions and researchers, despite the goal for sustainable industrialization promoted by the United Nations and the SDGs.

In the Italian context, the manufacturing building stock is characterized by several issues related to structural, technological, and environmental performance. Mainly because

of the dated construction periods of manufacturing facilities, the structural and technological solutions adopted have proven to be inadequate over time, and most of these facilities are not in line with the actual performance levels required for seismic response and energy and GHG emissions. On a national scale, manufacturing facilities account for 22% of the final energy demand considering both the operational phase of the facilities (i.e., lighting, heating, domestic hot water, and cooling) and the associated production processes. Despite these open and multi-faceted challenges, most of the studies retrieved in the literature concerning manufacturing facilities' heritage address only specific aspects [5]. Several studies have focused on the structural performance of buildings without considering the environmental impact of interventions or the possible improvement in energy performance by adopting specific technological and constructive solutions [6].

Notably, redevelopment interventions in manufacturing buildings necessitate thorough considerations to reconcile various conflicting aspects. In this regard, simulation and modeling techniques, which have become increasingly common and effective, can provide valid support. Moreover, when coupled with a parametric design approach at the beginning of the design process, they allow designers to make informed choices more easily and also exploit generative design procedures [7] that have been increasingly adopted in the construction sector as helpful instruments during the starting phase of the decision-making process. Choices made in the early stages greatly affect the overall quality of the final results, especially when a life cycle perspective is considered, ultimately aiming to enhance the energy and environmental performance of the built environment. All these tools also allow the incorporation of optimization analyses [8] and design-optioneering procedures [9], which are extremely helpful for the effective comparison and selection of different design alternatives, considering various criteria, such as economic, environmental, and energy aspects [10]. By leveraging software and plugins, designers can quickly generate and evaluate multiple design options, ultimately selecting the preferred one based on the project requirements. These kinds of support tools find applications in both defining retrofitting interventions and designing newly built facilities. In both these cases, buildings' internal layouts can be the main objective function of parametric studies, such as in the study by Eltaweel et al. [11], which compared 10 benchmarks to define the most cost-effective one for redeveloping a single-family house. Other researchers have proposed new approaches and methods for the evaluation of the environmental impact of buildings through the calculation of the embodied energy, trying to validate new open-access parametric software [12]. Studies focusing on specific building components are also available, addressing, for example, the envelope elements and air-conditioning systems [13].

Moreover, Bushra et al. [14], with an extensive review of the literature, highlight that most parametric studies are related to solar studies and indoor comfort issues, with building facades being the most explored components for parametric modeling applications. The latter has become particularly appealing for these studies given the diffusion of technological solutions such as building-integrated photovoltaics (BIPV) or building-applied photovoltaics (BAPV), which represent a possible improvement for a facility's external envelope, ameliorating, at the same time, the energy performance of the facility [15]. Cicelsky et al. [16] focused on physical and operational parameters to determine the optimal conditions for external facades to obtain free-running conditions in both winter and summer. Other researchers have integrated additional different topics into their studies considering biodiversity problems [17] or PV geometrical layouts in high-rise buildings [18]. In addition to social, environmental, economic and energy aspects, structural and constructive solutions have also been explored [19].

BIPV-related research is another promising field of application for optimization and parametric studies, although most of the available publications still focus on residential, office, and commercial intended use. Espitia-Mesa et al. [20] focused on the residential building stock, designing curved photovoltaic surfaces through a genetic algorithm (GA) to maximize the incident solar radiation, minimizing the occupied surface. As for office building type, studies were conducted in different countries and climate conditions.

Freitas et al. [21] performed a parametric analysis using Grasshopper to foresee BIPV integration in both roofs and facades for existing directional buildings in Brazil. Fu et al. [22] investigated the proper BIPV facade configuration (comparing three different schemes) for four different geometries of office buildings in China, demonstrating that the installation of this active technology can lead to significant energy savings. In line with previous research, Mitsopoulus et al. [23] proposed an optimization procedure to investigate the economic feasibility of a solar heating system, considering Greek buildings and different external insulation thicknesses and glazing types.

At the same time, lighting studies can be effectively performed using similar methodologies, as discussed in comprehensive review papers [11]. Qingsong et al. [24] evaluated the thermal behavior of an office building located in Beijing by integrating illuminance level calculations and energy demand evaluation. The implementation of optimization tools ensured the definition of the best window layout for each orientation to maximize useful daylight illuminance. Daylight availability within the indoor environment was also analyzed with respect to the parametric modeling and optimization of solar shading systems, as in the research by Alsharif et al. [25]. Similarly, Li et al. [26] conducted a parametric analysis to optimize external fixed solar shading devices, considering the user behavior patterns as influencing parameters in an office building.

In the literature, optimization analyses have been conducted with respect to industrial buildings, focusing primarily on production processes [27]. In the realm of building technologies, studies address specific components of the external envelope (e.g., skylights), which are strictly related to indoor thermal and visual comfort [28,29], but these studies often rely on traditional assessment methods.

As industrial facilities are usually not considered for this type of technological solution and research approach, this paper aims to evaluate retrofit solutions for existing industrial building facades. Generative design and optimization tools were applied in designing a BIPV system, as well as in the definition of shading solutions to be installed on the glazed portions, with energy, economic, and comfort aspects included as evaluation criteria. The proposed interventions aim to improve the energy and environmental performance of the existing industrial facilities during the operational phase, as well as enhance the indoor thermal and visual comfort conditions. Additionally, the suggested interventions for the external envelope of industrial buildings can also positively impact their aesthetic appeal, which is often characterized by low architectural quality due to the widespread installation of exposed precast concrete panels as cladding solutions. The method applied employs cutting-edge procedures and tools to overcome the limitations found in the literature regarding optimized configuration, which are sometimes still affected by burdensome or predetermined formulations [30].

The paper is structured as follows:

- Material and Methods (Section 2): detailed descriptions of the main procedural steps and simulation settings.
- Results (Section 3): presentation of the main findings for each topic addressed.
- Discussions (Section 4): analysis and comparison of the research outputs with similar studies in the literature.
- Conclusions (Section 5): summary of the research outcomes, along with an overview of the limitations and potential future developments.

2. Materials and Methods

The research was developed by implementing different optimization strategies and solutions to define possible retrofit configurations for existing industrial facilities and to evaluate their performance by adopting state-of-the-art simulation tools.

An existing manufacturing facility representative of the Italian industrial building heritage was used as an exemplary case study (Figure 1).

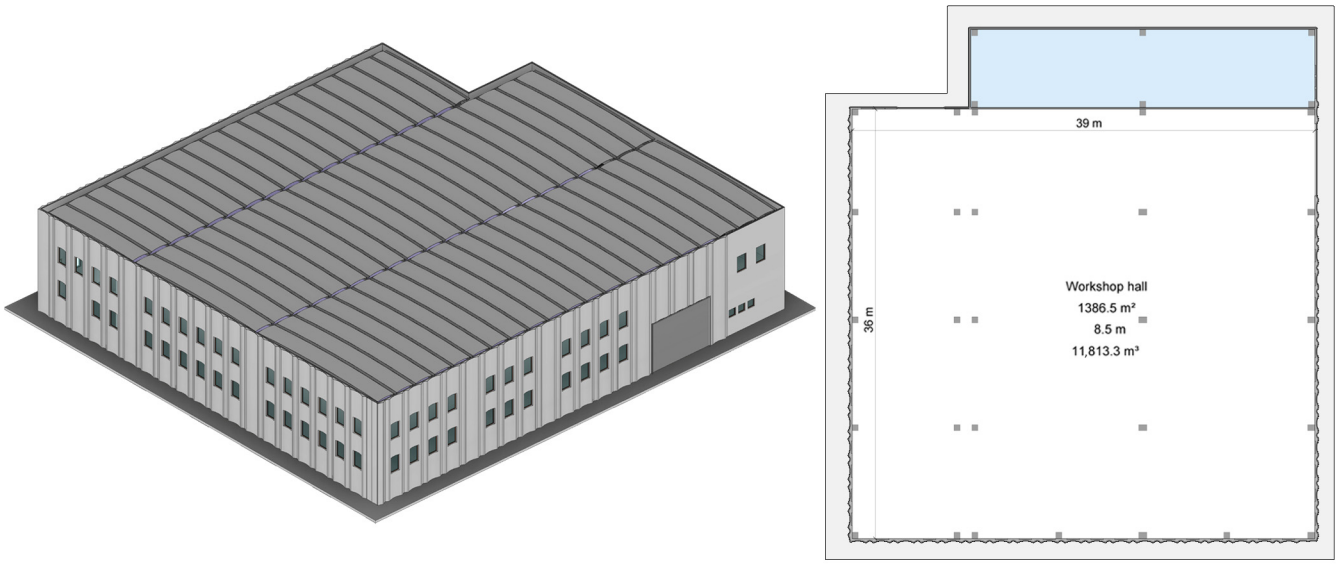

Figure 1. Three-dimensional model of the analyzed industrial building and ground floor plan. The blue area indicated in the internal layout is not addressed because it hosts a warehouse and archive on the ground floor and offices on the first one.

Given the poor architectural quality of these kinds of buildings, retrofit solutions aimed at enhancing their aesthetic performance, as well as improving their low energy and environmental standards, should be seriously considered. Therefore, some possible interventions were evaluated relating to multi-objective optimization studies and daylight performance assessments. These interventions included the installation of BIPV facades and the implementation of external louvers on south-facing openings to reduce indoor summer overheating. The overall procedural framework is outlined in Figure 2.

The main methodological steps are reported below:

- At first, the building was accurately modeled in a BIM environment using Revit, based on detailed specifications of the geometry and internal layout retrieved from the original design drawings and on-site inspections. This model represented the starting point for all subsequent applications and assessments in the research.
- The interoperability between Revit and Rhinoceros Grasshopper was exploited to directly import the building's geometry and apply a series of autonomously drafted Visual Programming Language (VPL) algorithms. These were designed to effectively intertwine the input data and outcomes of the different parts of the script leveraging the multidisciplinary simulation tools. Figure 3 shows the script created by the authors.

The main sections are highlighted to point out the key tasks addressed in detail. The crucial topics can be schematically synthesized as follows:

- The Ladybug plugin and its components were used to import and analyze the climatic data referring to the Florence area and to conduct solar and radiation analyses. Simulations were carried out for both the summer and winter solstices (21 June and 21 December) considering a time interval between 7:00 a.m. and 6:00 p.m. to align with the working hours of the company occupying the building. To promote simultaneous energy production and consumption, it is advisable to maximize the yield of the photovoltaic system during the operating hours of the machinery and installed equipment. A multi-objective optimization study was carried out using the Octopus plugin [31] to evaluate different BIPV layouts applied to the different building facades. The energy production and initial investment costs were addressed as evaluation criteria. To express both parameters, the total incident radiation and the total area of the panels installed were used as references. The former is key for assessing the productiveness of the installed PV system, while the area of the PV surface was assumed as representative of the costliness of the different configurations evaluated, as

it is directly related to the number of panels installed. Solar incident radiation was calculated through the dedicated simulation engine provided by the Ladybug plugin and included in the Octopus-based optimization. The tilt angle (ranging from 0° to 90° with 10° increments) and the distance (ranging from 0.5 m to 1.5 m in 0.20 steps) between consecutive rows of PV modules on each facade were introduced as the variables for the problem (Table 1). The minimum distance was set to avoid the overlapping of panels when considering their perfectly vertical layout. The research was further developed by applying progressive rotations of 10° with respect to the N-S axis for the entire building, considering the PV modules arranged according to the optimized configuration minimizing the panels' area in winter conditions. This approach aimed to identify the most promising building orientation ranges for implementing BIPV solutions.

- The Honeybee plugin [32] was used to assess the visual comfort conditions within the working environment, and it was exploited to perform daylight simulations considering the daylight factor (DF), daylight autonomy (DA), and the useful daylight illuminance (UDI) as reference parameters. These parameters respectively represent the amount of daylight that penetrates the building interior, the extent to which a space is naturally lit during occupied hours to satisfy the required illuminance conditions, and the percentage of the annual hours during which the illuminance threshold is met. Solar radiation and climate data were derived from those imported using Ladybug, as previously introduced. To account for the different possible configurations of the building's apertures commonly retrieved in existing manufacturing facilities, alternative configurations were evaluated: windows on each facade arranged in a single row or two rows, and the presence of roof skylights, including a combination of these scenarios. In this case, the simulations were performed considering the entire year and a minimum illuminance level of 300 lux, as prescribed by UNI EN 12464-1 [33] for generic activities in an industrial environment.
- The outputs of daylight illuminance and incident radiation analyses were also included in defining the optimized solar shading system configurations. In this case, different alternative solutions were evaluated using a design-optioneering approach, iterating a series of simulations through the Colibrì plugin [34] for Grasshopper. For this analysis, 0.20 deep external louvres were designed, considering the tilt angle of each blade ranging from 0° to 90° and vertical spacing between consequent slats from 0.20 m to 1 m. The evaluation focused on 60 distinct options, each resulting from variations in the geometrical arrangements achieved through adjustments of 10° in blade tilt and 0.20 m in vertical spacing. These alternatives were assessed for their performance during the summer solstice throughout the occupancy period. The results were explored through the online viewer Design Explorer by Thornton Tomasetti [35], which allows the comparison and filtering of different configurations tested according to the desired outputs or limitations assigned to the design variables. For the study here presented, the amount of solar incident radiation and the internal UDI average values were considered driving design factors, aiming for an arrangement capable of preventing the influx of excessive solar radiation without compromising adequate natural lighting contribution.

The results obtained for both the BIPV layout and louvres' configuration were further evaluated through dedicated energy simulations carried out using Design Builder. The single thermal zone geometry was exported from the Revit model to serve as the base for the new energy model in the Design Builder environment. This model was enriched with a set of information retrieved from in-situ surveys and the indications directly provided by the company (the opening time, occupation profile, indoor air temperature setpoint, and system equipment). The external envelope technological solutions and thermal properties of each envelope component were properly modeled according to the original drawings and available technological details. The main settings used for the energy model are summarized in Table 2. Notably, the internal loads were neglected in the energy balance of

the building because the currently hosted company operates in the light mechanic sector without any highly emitting machinery. The energy simulations were performed adopting the simple HVAC method directly proposed by the software, and they were carried out to compare the energy consumption profile of the building for a winter design day with the production ensured by the previously outlined optimized BIPV implementation. Flexible PV panels were considered, and their characteristics are detailed in Table 3.

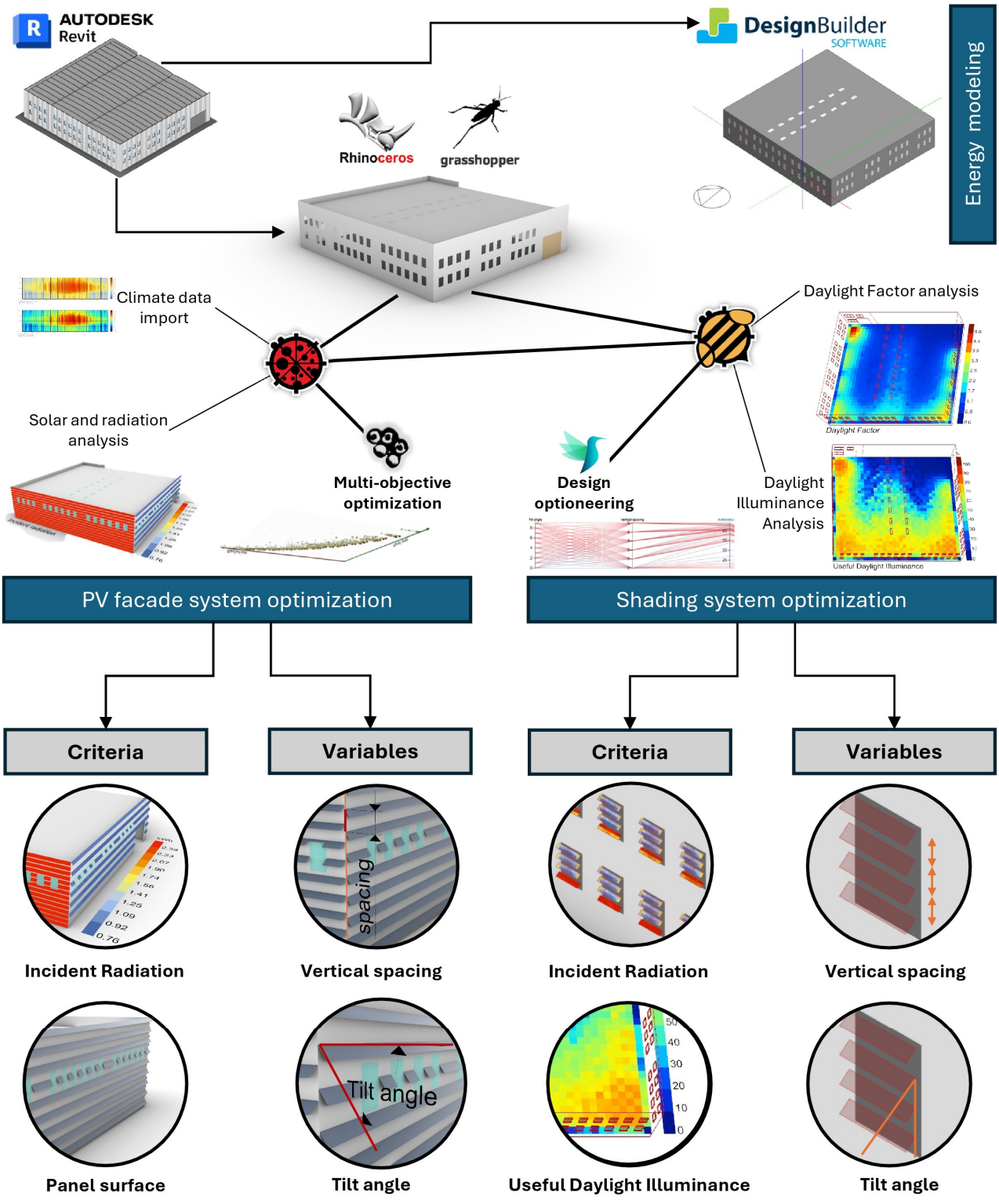

Figure 2. Flow chart of the methodology.

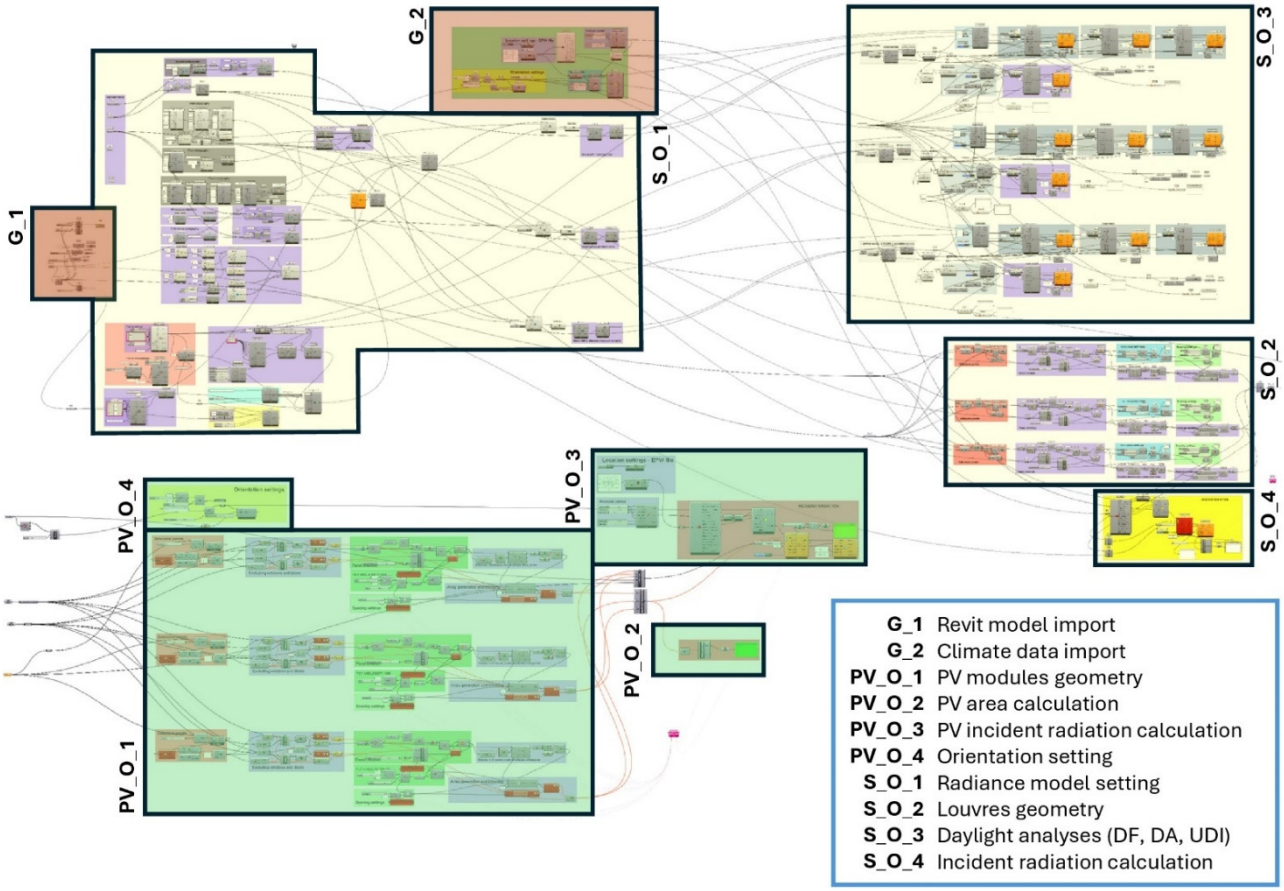

Figure 3. Visual Programming Language (VPL) script developed by the authors for the purposes of this study. Each of the boxes represents a different algorithm section for a specific purpose. To ensure a more effective comprehension of the script, thematic grouping is provided. The boxes highlighted in orange refer to general tasks (G), propaedeutically developed for all the following phases. The green boxes include the tasks addressing PV optimization (PV_O), and the yellow ones refer to the shading system optimization (S_O).

Table 1. Parameters setting for simulations and optimization in the Grasshopper environment.

Element	**Dimensions**	
PV panel	1.09 m	0.58 m
Louvres blades	1.10 m	0.20 m
Parameter	**Range**	**Increment**
PV vertical spacing	0.5–1.5 m	0.20 m
PV tilt angle	0–90°	10°
Louvres vertical spacing	0.20–1 m	0.20 m
Louvres tilt angle	0–90°	10°

Table 2. Parameters setting for the energy model in Design Builder.

Parameter	**Value**
Heating setpoint	18 °C
Occupancy time	8:00–17:00
Occupancy	0.01 people/m^2
Metabolic rate	167 W/person
Natural ventilation flow rate	0.77 m^3/s
Airtightness	0.20 ac/h
Sheltering coefficient	0.7

Table 3. Flexible PV panel characteristics.

Parameter	Value
Maximum power	110 W
Maximum power voltage	19.6 V
Maximum power current	5.66 A
Module efficiency	17.29%
Operating temperature	−40 °C to 85 °C
Type of solar cell	Monocrystalline silicon cells
Cell size	166 × 83 mm
No. of cells	36
Temperature coefficient of Voc	−0.28%/°C
Temperature coefficient of Isc	0.02%/°C

Energy simulations were also carried out to assess the impact of the window louvres on indoor temperature during a summer day. Once again, 21 June was chosen in this case. The influence of the installation of solar shading systems was evaluated by comparing different configurations included in the design-optioneering procedure.

Case Study Building

The industrial building chosen as a case study is located in an existing industrial district in the Casentino Area in Tuscany (Central Italy), in the Municipality of Subbiano, province of Arezzo. It is situated in climate zone D [36] with 2041 heating degree-days (HDD), and it is characterized by a temperate climate (zone C) according to the Koppen classification. The main climate characteristics are illustrated in Table 4.

Table 4. Climate data for Florence. In the table: HDD means heating degree days, GH stands for global horizontal radiation, Dh means diffuse radiation, Bn means direct normal radiation, Ta stands for air temperature, Td stands for dewpoint temperature, and Ws means wind.

Latitude	Longitude	Climate Zone	Heating Period	HDD [K/d]	Gh [kWh/m^{2}a]	Dh [kWh/m^{2}a]	Bn [kWh/m^{2}a]	Ta [°C]	Td [°C]	Ws [m/s]
43.34° N	11.52° E	D	1/11–15/04	2041	1447	629	1496	15	7.9	2.8

The representative case study building analyzed is a single-story facility built in the 1990s. This typological variant has been widely observed throughout the Tuscany Region and the whole national territory, as it features the most recurrent constructive and technological solutions adopted between the 1970s and 1990s. The facility is characterized by a rectangular shape with the following main dimensions: 36 m × 38 m. The gross area is about 1400 m^2, and the volume is equal to about 11,900 m^3, considering an average internal height of 8.50 m. The load-bearing structure is made of portal frames made by precast concrete tenon head columns and precast-prestressed H-shaped beams. The load-bearing structure is completed by roofing Y-shaped beams. The external walls are made of lightened precast concrete sandwich panels (0.13 m thick), while the roofing layer consists of external curved fiber–cement panels and an internal insulated false ceiling. The windows are mainly located on the southern, western, and eastern orientations due to the presence of an adjacent office building block. This is a recurrent scheme for this building typology. The main distinguishing thermal properties of the external envelope are illustrated in detail in Tables 5 and 6. For the insulation layer, half the thickness of the insulation material is considered for the energy simulation to consider its possible decay over time. This was assumed for both the external wall precast panels and roof existing stratigraphy. As regards the heating system, it is made of fan heaters with a traditional and outdated gas boiler as a generation system (η = 0.6). No mechanical ventilation system or cooling is installed in the working area. The existing heating system has been modeled to validate the energy simulations with respect to the available energy bills. Subsequently, for the

comparison between the building's energy needs and the PV panels' production, a heat pump characterized by a coefficient of performance (COP) equal to 3.5 is considered.

Table 5. Stratigraphy and main properties of the external walls. In the table, half the thickness of the insulation material is indicated.

Material	Thickness (m)	Conductivity (W/m·K)	Specific Heat (J/kg·K)	Density (kg/m^3)
Precast concrete	0.02	2.07	1000	2400
Insulation material (EPS)	0.045	0.04	1450	15
Precast concrete	0.02	2.07	1000	2400

Table 6. Stratigraphy and main properties of the roofing elements. In the table, half the thickness of the insulation material is indicated.

Material	Thickness (m)	Conductivity (W/m·K)	Specific Heat (J/kg·K)	Density (kg/m^3)
Asbestos–cement tiles	0.01	0.6	1000	1800
Glass wool	0.06	0.04	1030	12
Air gap	0.55	-	-	-
Asbestos–cement tiles	0.01	0.6	1000	1800

The existing windows are made of metal frames without a thermal break, and the glazing portions are characterized by the following visual and thermal properties: thermal transmittance = 3 W/m^2·K, solar factor = 0.6, light transmittance = 0.4. Regarding the existing polycarbonate skylights, they are characterized by the following features: thermal transmittance = 2.8 W/m^2·K, solar factor = 0.35, light transmittance = 0.4.

3. Results

The results are presented in this section, discussing the outputs of each methodological step in separate subsections, aiming to present them effectively and concisely.

3.1. Optimization of the PV Panels' Distribution

The first stages of the research revolved around the definition of the optimized layout for integrating PV panels in the building's facades. The results reported in Figure 4 refer to the optimization of the summer performance: on the Y axis, the area of the modules is reported, while the incident radiation is accounted for in the X direction, and it was expressed with its inverse value, since the optimization algorithm works with minimization criteria.

In the graph, the Pareto front can be retraced, and it the solutions belonging to it are highlighted in red. These configurations represent the "non-dominated" solutions, meaning they are superior or equal to all other alternatives in at least one objective without being worse in any other. For this reason, they represent the best possible trade-offs between conflicting objectives; therefore, deeper considerations focused on them. Solutions *a* and *f* in Figure 4 are representative of the extreme opposite conditions, with the former maximizing the PV panels' surface and the latter minimizing it. As expected, the installed PV surface and the total incident radiation are inversely proportional. Configuration *a* is characterized by 0.5 m spaced rows of PV panels, tilted at 75° on the east and west facades and 50° on the south one. It had the highest value of the installed PV surface area, totaling 963 m^2 with an incident solar radiation of 3356 kWh. This distribution ensures an enhanced level of incoming radiation compared to a hypothetical configuration with facades completely covered with vertical PV panels; in this case, the solar incident radiation would decrease by about 14% (2904 kWh). However, from an exclusively construction point of view, the installation of vertical panels is easier than tilted ones because the supporting sub-structure would be substantially simplified. Intermediate configurations (*b*, *c*, *d*, and *e*) denote compromise solutions between the extreme conditions outlined earlier. Solutions

c, *d*, and *e* differ by approximately 200 kWh in total incident radiation. It is worth noting that these intermediate configurations present the same tilt angle and spacing for the east and west facades, while for the southern facade, there is a reduction for both parameters. Furthermore, configuration *b* presents the lowest spacing for the west facade equal to 0.5 m. In contrast, solution *e* provides the highest one, equal to 1.3 m, for the eastern and western facades.

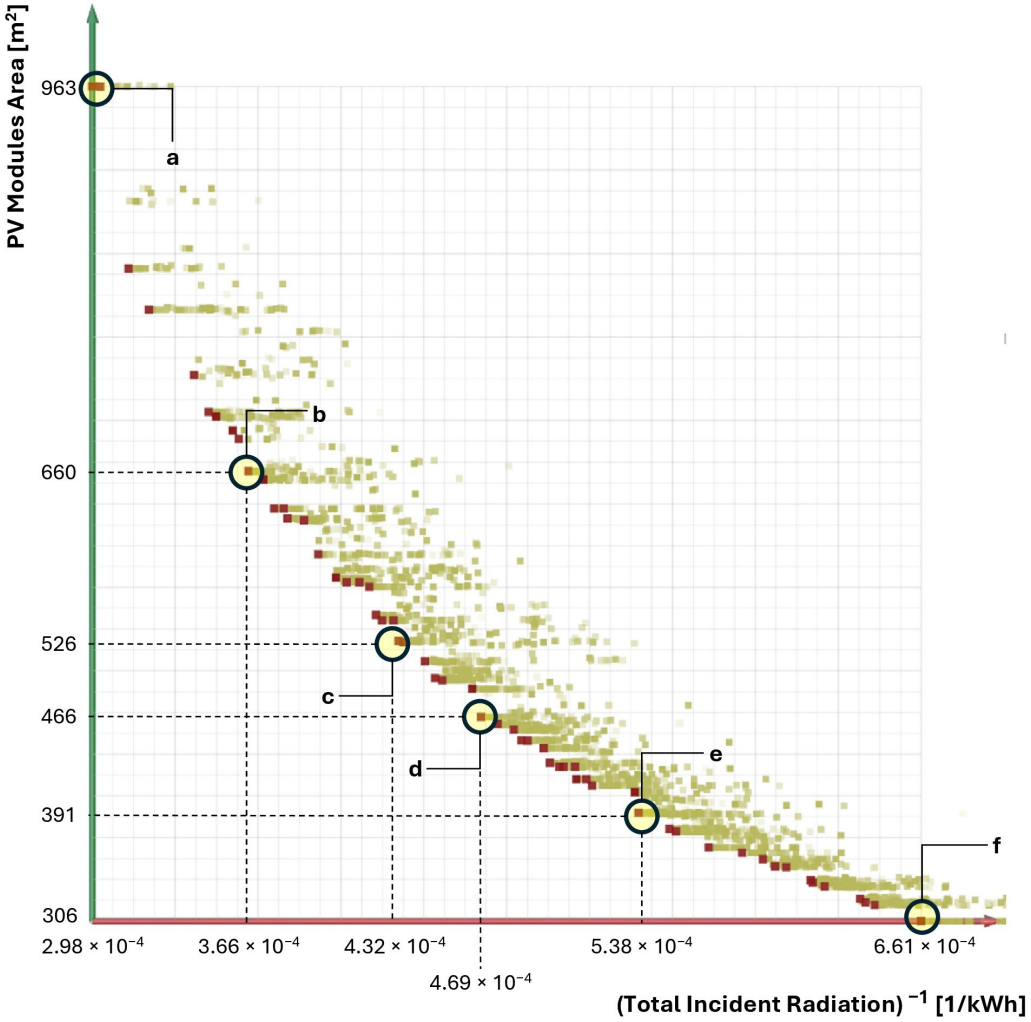

Solution	East Facade		West Facade		South Facade		PV Modules Area	Total Incident Radiation
	Tilt	Spacing	Tilt	Spacing	Tilt	Spacing		
a	−75°	0.5 m	−75°	0.5 m	−50°	0.5 m	963 m²	3356 kWh
b	−45°	0.9 m	−75°	0.5 m	−25°	1.1 m	660 m²	2729 kWh
c	−45°	0.9 m	−45°	0.9 m	−25°	1.1 m	526 m²	2313 kWh
d	−55°	1.1 m	−55°	1.1 m	−25°	1.1 m	466 m²	2133 kWh
e	−45°	1.3 m	−45°	1.3 m	−25°	1.1 m	391 m²	1859 kWh
f	−35°	1.5 m	−35°	1.5 m	−35°	1.5 m	306 m²	1512 kWh

Figure 4. Pareto curve related to the optimization of the PV panels' layout for the summer solstice.

Notably, solution *d* emerges as particularly favorable: here, the south-oriented facade features a higher concentration of modules tilted at steeper angles, enhancing solar capture compared to the generally less productive west and east facades. Solutions *d* and *e* only differ in terms of the vertical spacing of the PV modules' rows, equal to 1.1 m and 1.3 m, respectively. Configuration *d* appears to be preferable as an increase in the PV surface of about 16% obtains a rise in the solar radiation capture potential of around 17%.The same procedure was replicated for the winter design day (21 December), and the outcomes are synthesized in Figure 5. In this case as well, solutions *a* and *g* are the limit conditions, respectively maximizing and minimizing the PV panels area. For the winter season, the tilt angles on all the facades tend to be closer to the vertical position due to the lower solar height. Solution *a* foresees a PV panel area equal to 963 m^2 with incident solar radiation equal to 1298 kWh. Compared to the complete PV cladding of the external walls, the reduction in incident solar radiation is limited to about 6%. To understand the contribution of each facade to the total solar radiation some further considerations are needed. The southern-oriented facade alone can capture 65% of the total solar incident radiation and installing PV modules on this side could be reasonable in case of a limited investment budget available. Point *g* represents the opposite limit configuration, minimizing the PV panel area and consequently reducing the amount of incident solar radiation by about 32%. As introduced before in the case of the summer study, compromise configurations (*b*, *c*, *d*, *e*, and *f*) are characterized by an intermediate performance compared to the limit solutions. Layout *f* presents about half (555 kWh) of the total incident solar radiation compared to configuration *b* (1153). Except for solution *b*, the others are characterized by the same tilt angle equal to -70° and a spacing of 1.5 m as regards eastern- and western-oriented facades. For the south orientation, the configurations present significant variability for both parameters, registering the lowest value for the configuration *b* and the highest one for *f*. The highest difference in incident solar radiation is between *c* and *d*, equal to about 340 kWh.

Also in this case, configuration *d* can be considered as the advisable one, with a total installed PV panel area equal to 450 m^2 and an incident solar radiation of 761 kWh. In this intermediate configuration, the geometrical layout of the southern-oriented PV panels significantly affects the amount of the incident solar radiation.

To evaluate the energy production potential of the BIPV modules arranged according to the chosen configuration (*d*), a dedicated Design Builder model was produced, where the geometry of the solar collectors was modeled, and their technical settings were introduced. In Figure 6, the achieved energy production is reported along with the lighting and heating demand over the winter period (1 November–31 March). The data are reported for monthly, daily, and hourly distribution considering the whole period, the month of December, and a specific design week including 21 December. As shown in the graphs, the energy production provided by the facade-mounted PV panels is not enough to cover the building's energy demand during the entire winter period, except in March, when the peak of production (~3900 kWh) is registered. As detailed at the daily level, during weekends, the interruption in the working activity determines a surplus generation to be stored or financially rewarded through the cession grid mechanism. The graph at the hourly level allows to consideration of the simultaneous generation and related energy demand. During the peak energy demand hours corresponding to the beginning of working activities, the PV modules are unable to cover the required energy needs. A shift in the peak of energy production (central hours of the day) and the peak of energy demand occurs. Hence, the installation of PV modules on the facades should be possibly coupled with PV panels installed on the roof floor to exploit the larger surface available and maximize the energy generation.

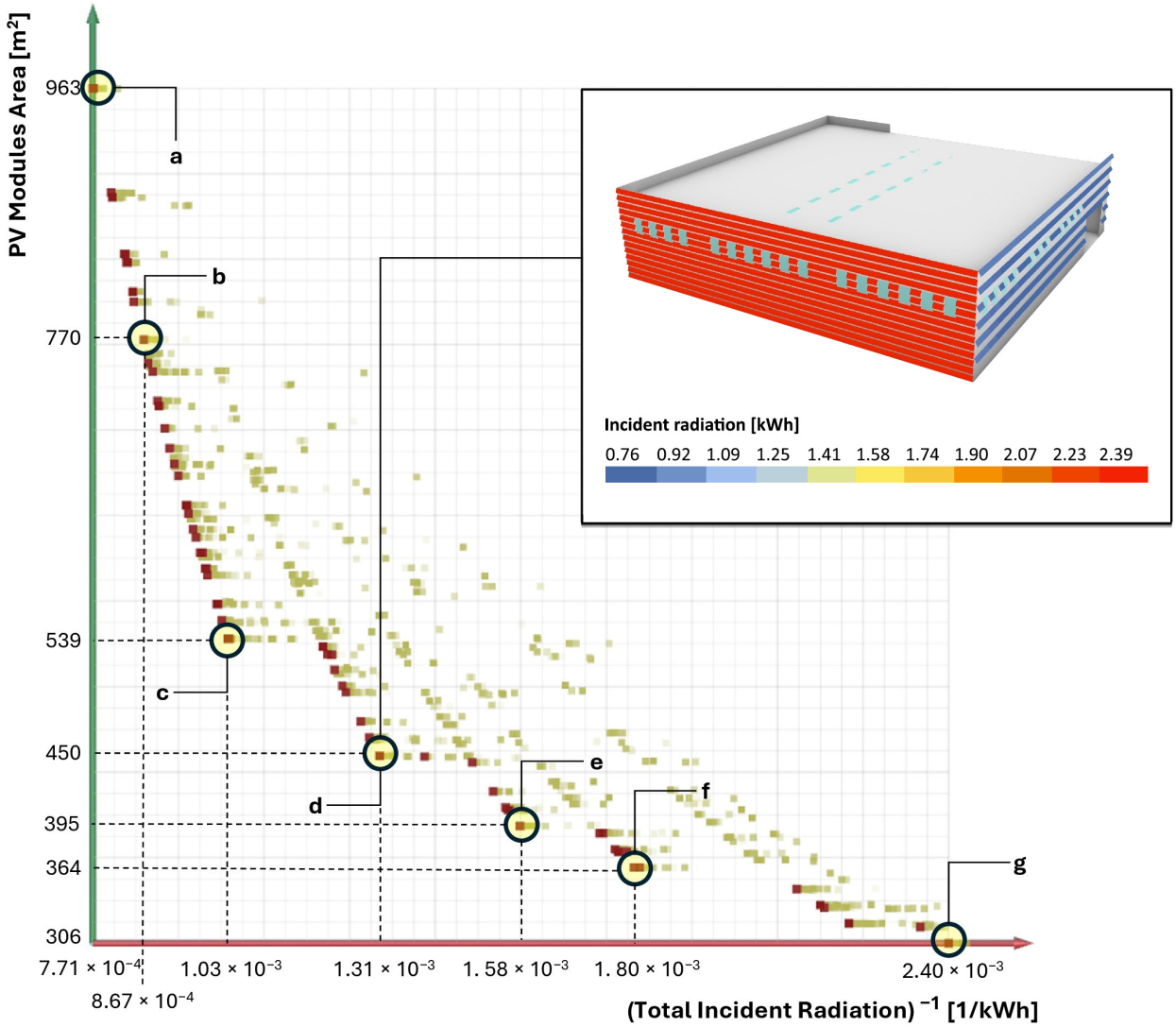

Solution	East Facade		West Facade		South Facade		PV Modules Area	Total Incident Radiation
	Tilt	Spacing	Tilt	Spacing	Tilt	Spacing		
a	−70°	0.5 m	−75°	0.5 m	−75°	0.5 m	963 m²	1298 kWh
b	−70°	1.3 m	−75°	0.5 m	−75°	0.5 m	770 m²	1153 kWh
c	−70°	1.5 m	−70°	1.5 m	−70°	0.5 m	539 m²	970 kWh
d	−70°	1.5 m	−70°	1.5 m	−75°	0.7 m	450 m²	761 kWh
e	−70°	1.5 m	−70°	1.5 m	−75°	0.9 m	395 m²	632 kWh
f	−70°	1.5 m	−70°	1.5 m	−70°	1.1 m	364 m²	555 kWh
g	−70°	1.5 m	−70°	1.5 m	−70°	1.5 m	306 m²	417 kWh

Figure 5. Pareto curve related to the optimization of the PV panels' layout for the winter solstice.

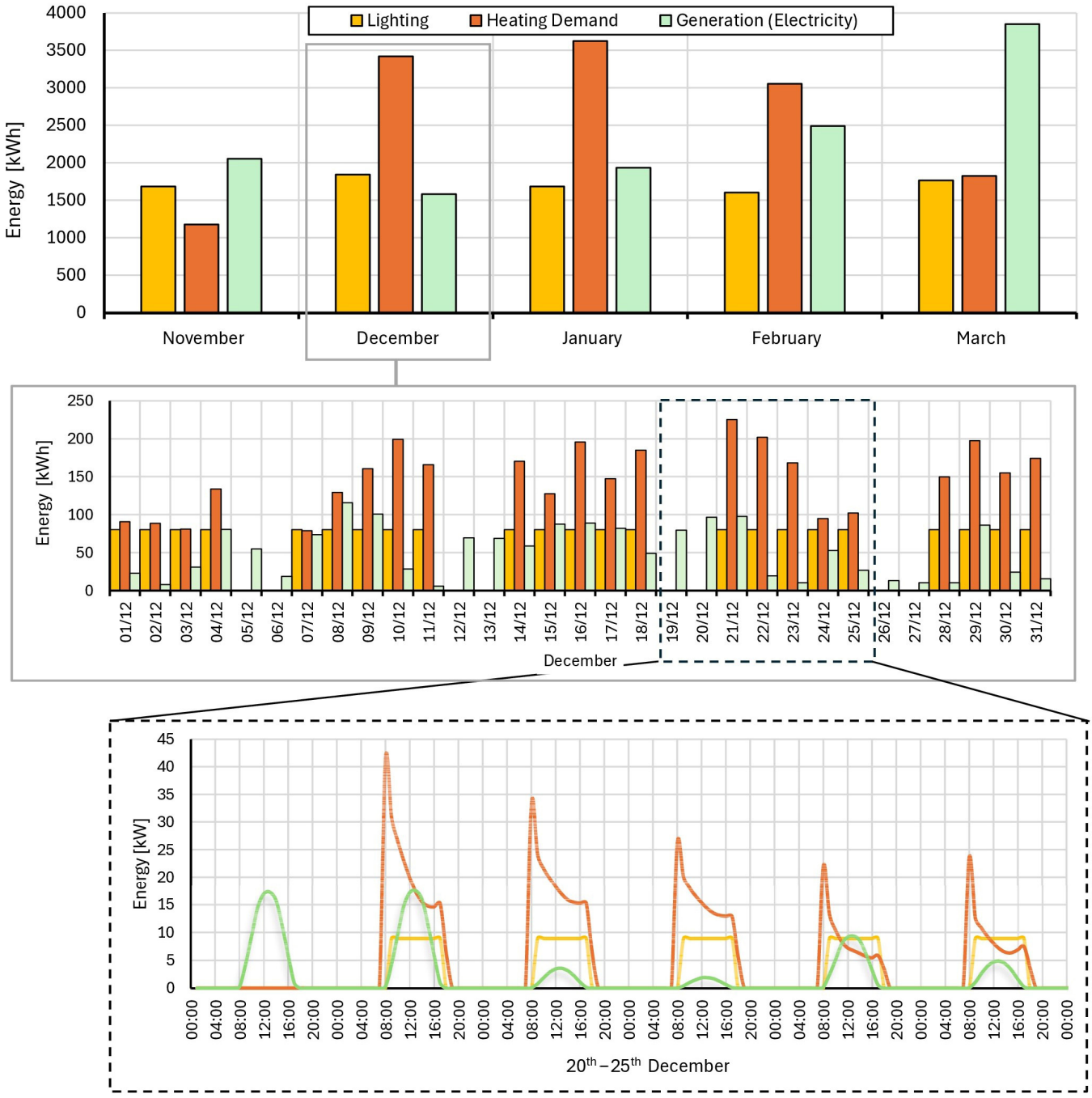

Figure 6. Industrial building energy needs and PV panels' production in the advisable configuration for winter, the month of December, and a winter design day.

Once the optimal distribution of the PV modules was considered, the analyses were extended to evaluate the influence of the building's orientation on the final results. The main outcomes are proposed in Figure 7. As emerging from the graph, buildings with orientations ranging from south–east to south–west present the highest solar exploitation potential, with the maximum incident radiation obtained at a 20° east rotation.

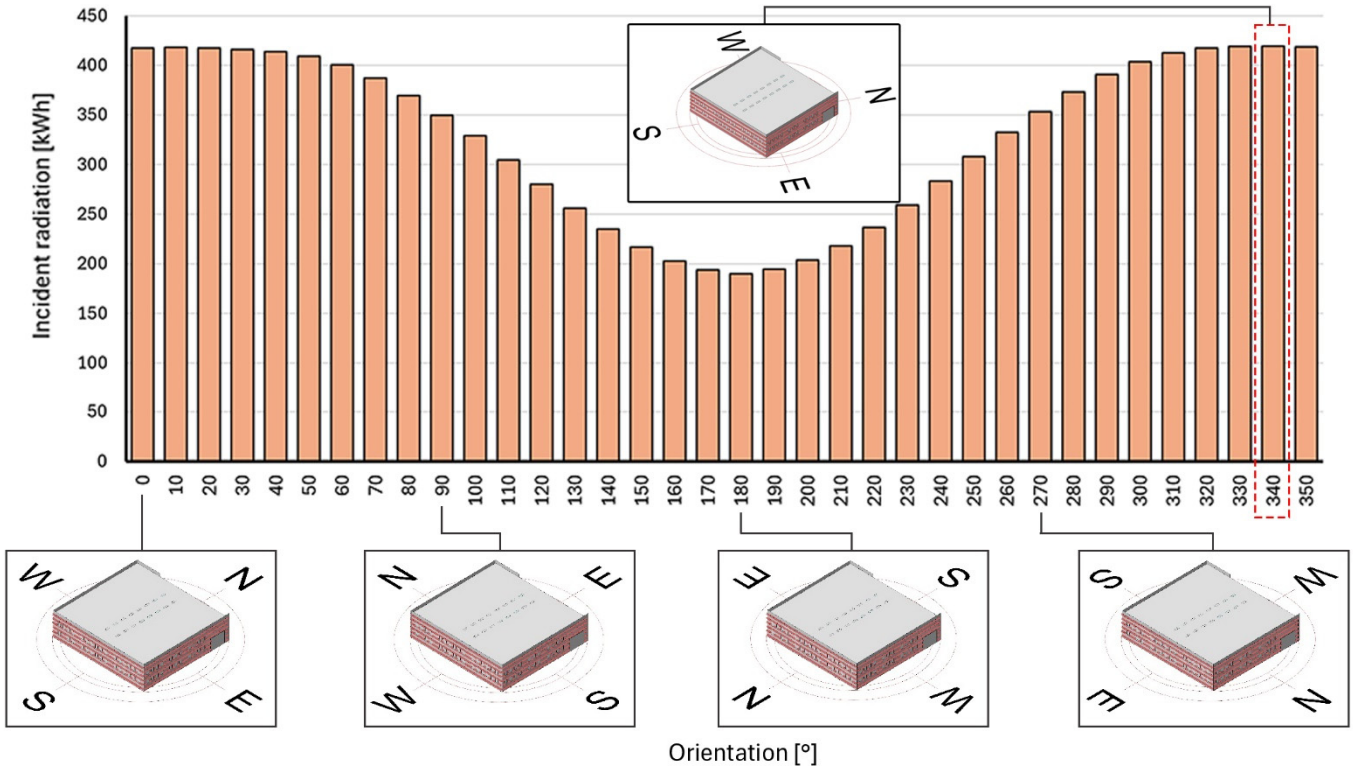

Figure 7. Building orientation study.

3.2. Daylight Analysis

Figure 8 illustrates the spatial distribution within the working environment of the DF, DA, and UDI values. In this case, possible variations in the base case buildings were included, aligning with the configurations commonly found in the existing built heritage. A single row of windows is not adequate in the case of facilities with such a wide internal volume. The working environment is characterized by a DF ranging from 0.08 to 1.6%. In addition, in almost the entire working area, the UDI threshold is not reached for more than 50% of the time over one year (1309 points over 1330, obtained considering a square meshing with 1 m side). In general, observing the lighting maps, it is evident that the UDI decreases with the increasing distance from windows, as confirmed by other authors in the literature [37]. For this reason, the WWR (window-to-wall ratio) tested is not sufficient given the building's dimensions. A general decrease in each parameter considered (DF, DA, UDI) occurs when the opening percentage located in the external envelope decreases. This is highlighted also by findings outlined by other authors in the literature [38]. The average DF rises for the configuration with two rows of windows, and it is equal to 1.12%. The configuration with two rows of windows on each facade and the presence of skylights on the roof slab proves to be the most effective one in terms of visual comfort. More appropriate UDI levels are registered in the central part of the building, with values ranging from 40% to 70%, due to the apertures above. In this case, the number of points characterized by the UDI value below the threshold for 50% of the time over one year is lower and equal to 627. It is worth noticing that only the portion near the windows ensures a proper value of the DF, higher than 2.2%. For this reason and comparing the outcomes obtained for both the DA and UDI in the three evaluated scenarios, it is possible to affirm that the presence of skylights affects the visual comfort parameters to a lower extent than the windows.

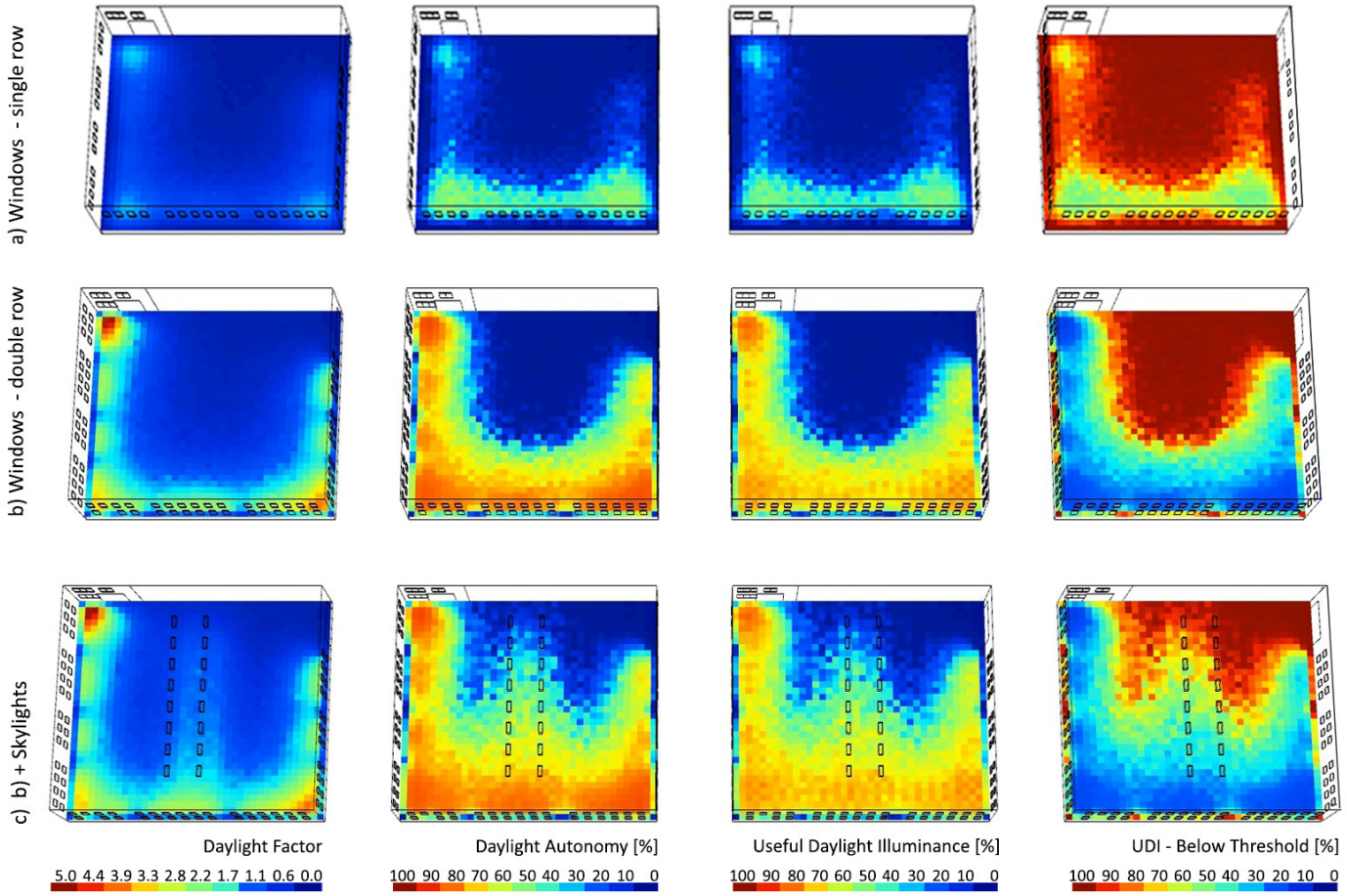

Figure 8. Spatial distribution of the DF, DA, UDI, and UDI below threshold within the working environment according to the different window and skylight distributions.

3.3. Optimization of Solar Shading Systems

The investigation of the solar lighting conditions was extended to include the design of a solar shading system design for the south-oriented windows. Reference was made to the actual layout of the case study facility, which features a double row of windows and roof skylights. In this case, a design-optioneering technique was applied to identify the best-performing configuration by analyzing the configurations generated by varying the input parameters. The limited number of alternatives to be evaluated allowed for a manual filtering and selection procedure, as presented in Figure 9, according to the visualization scheme proposed by the Design Explorer tool. This approach was adopted to evaluate, filter, and rank the configurations of interest. In particular, the five most promising solutions are highlighted from the total number of the possible configurations generated, as detailed in the figure. As emerged from the graph, acting on the columns allows for filtering the layout produced to impose a threshold range for both the UDI and incident radiation. Considering the high values of incident radiation on the louvres and the acceptable natural daylight, solutions with horizontal (or nearly horizontal) blades variously spaced as shown in the five examples reported in the figure, should be preferred. Since the design-optioneering simulations were performed for the summer solstice conditions, the horizontal overhangs maximize the solar radiation during the summer without preventing natural lighting during the other seasons when solar radiation is preferable for lighting purposes. As shown in the graph in Figure 9, combining the values of the first and second columns, the performance in terms of both the UDI and incident solar radiation can be retrieved in the third and fourth columns. The solar shading effect is enhanced when reducing the vertical spacing up to 0.20 m with horizontal slats. Increasing the distance between subsequent

shading blades results in better UDI levels, ranging from 35% to 40%. On the other hand, layouts characterized by steeper tilt angles over 45° are expected to compromise visual comfort quality as the average UDI falls below 25%, and the solar shading during the summer appears to be not as effective.

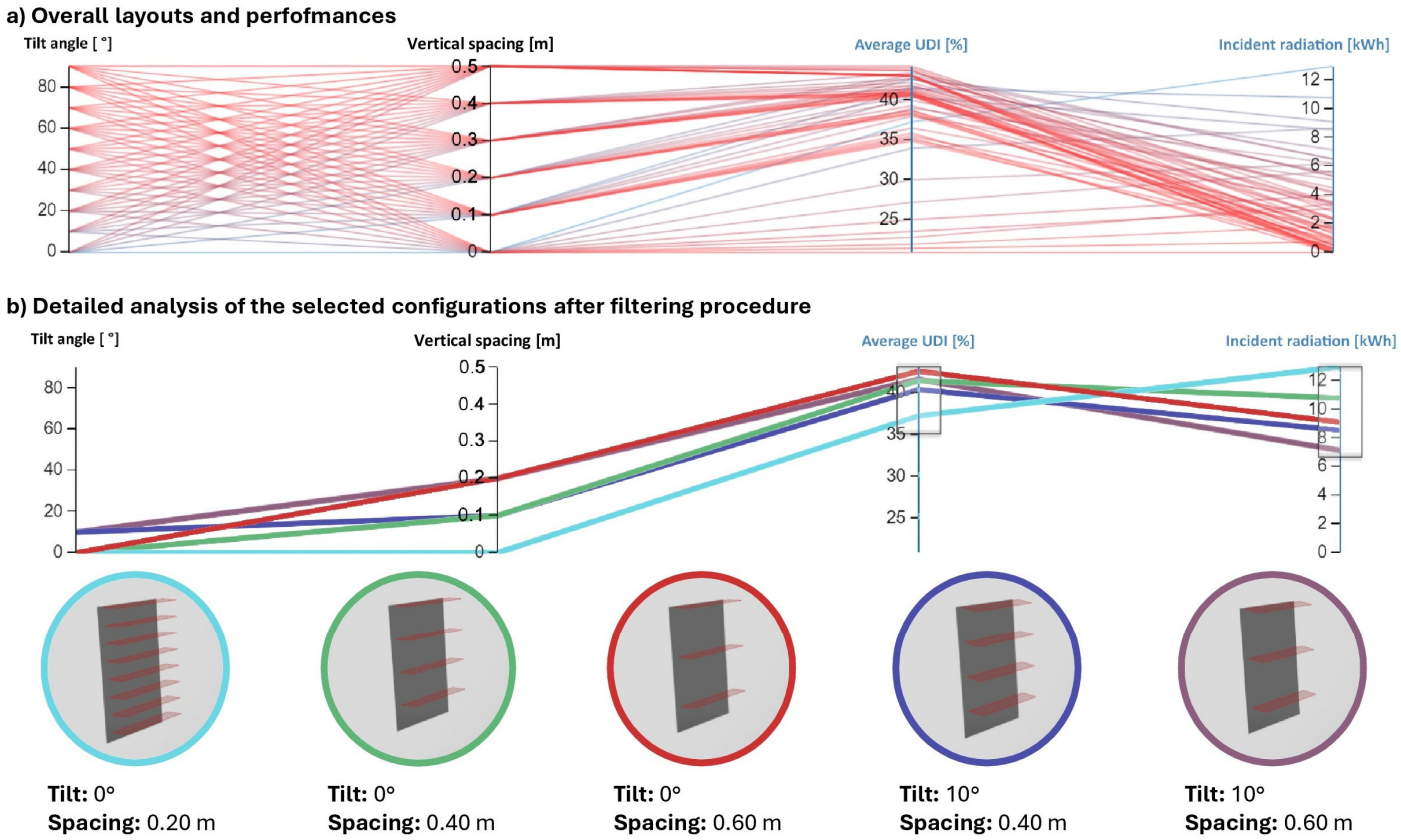

Figure 9. Results visualization in Design Explorer: first, the total number of possible configurations is presented to later extract the solutions of interest for the final goal of the research. These five layouts are also graphically represented to better show their geometries.

To evaluate the effectiveness in reducing summer overheating conditions, specific simulations were performed using Design Builder. The base case building without any solar shading and configurations (1) and (4), previously introduced, were analyzed in terms of the indoor air temperature. The findings of this assessment are reported in the graph in Figure 10. As illustrated in the graph, both shading solutions have comparable results in terms of the indoor temperature reduction, with a slight preference for layout (1), as could be anticipated from the previous results of the optioneering studies. The effect of the louvres is more appreciable during the central hours of the day, with a peak reduction of about 0.46 °C achieved from 13:30 to 14:00 and an average value of 0.39 °C considering the entire afternoon. The difference between the two configurations is limited, as the average reduction achievable for configuration (4) is equal to 0.36 °C. This second solution should be preferred considering its more promising performance in terms of the natural lighting conditions and the reduced number of components to be installed.

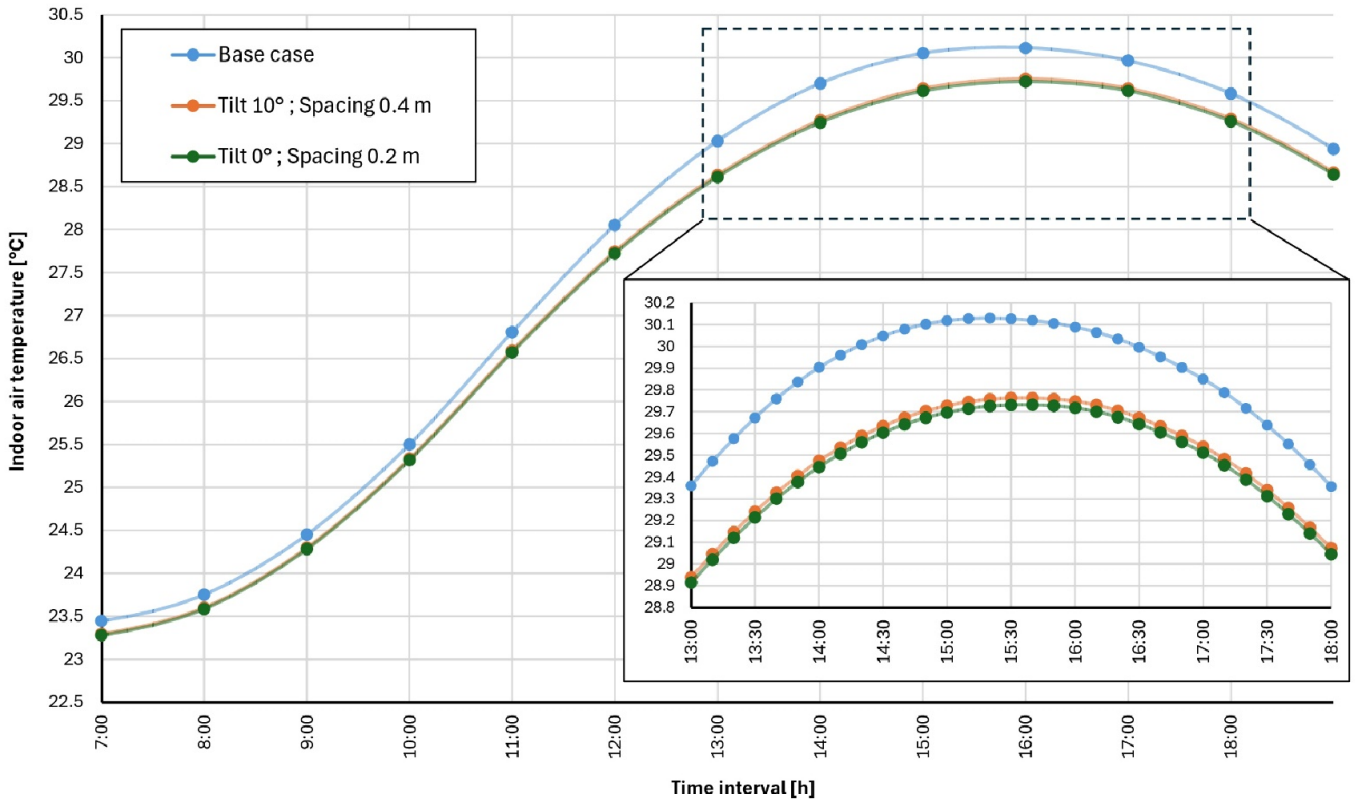

Figure 10. Trend of the indoor air temperature for the base case (current thermal conditions) and solutions (1) and (4) with the installation of solar shading systems for the southern orientation.

4. Discussion

Considering the results related to the facade orientation and the installation of PV modules, buildings oriented between south–east and south–west are characterized by the highest solar exploitation potential, with a pick obtained for the 20° east rotation. Similarities can be found in the literature. For instance, Chivelet et al. [39], evaluating back-ventilated BIPV facades, conclude that the most promising facade orientation for producing electrical energy is south-oriented. This result is also confirmed by Reffat et al., who conclude that, considering different PV coverages on facades, the south- and east-oriented facades are the most productive [40].

Coming to the PV module layout, the optimal tilt angle ranges from −35° to −75° for the two solstice days considered. These results are aligned with the findings of similar studies in the literature. Paydar et al., analyzing overhang shaders of 0.50 m, affirm that for the winter season, the cost-effective solution foresees the tilt angle equal to −60° [41]. This geometrical layout is similar to the optimized configuration (*a*) for the winter solstice determined in our research. This solution (*a*) presents a tilt angle ranging between −70° and −75° and spacing equal to 0.5 m for the east, west, and south facade, with a maximum incident solar radiation equal to 1298 kWh, corresponding to 963 m^2 of PV panels installed. Some research in the literature pointed out that tilted and movable configurations of PV panels can significantly enhance renewable energy production compared to fixed ones (ranging from 7% to 30%) [40]. The choice of the geometrical configuration for similar BIPV solutions to be adopted on manufacturing facility facades should also consider the energy demand of the industrial facility and the possible fluctuation over the year.

The integration of PV panels on different facades of manufacturing buildings certainly requires some considerations about feasibility and constructability, accounting for possible constraints and limitations such as the presence of the maneuvering, loading, and unloading spaces, as well as site-specific factors that may limit the available area for PV panel installation. This is strictly linked to the geometry and depth of the PV panels: increasing

the size of the modules requires additional consideration of the self-shadowing effect [42]. Finally, from a structural point of view, the installation of similar systems may result in an undesired increase in permanent loads when fixed directly on the external walls, whose considerable mass is a detrimental factor in the case of seismic actions [43].

Other limitations can be represented by the effective availability of commercial technological solutions capable of replicating the optimized configurations obtained from the performed simulations. Usually, the technological and constructive systems available on the market for integrating PV panels into building facades are limited only to specific tilt angles or precise tilt ranges that may not be the optimal ones. The analyses presented in this work proved that the range of proposed solutions differs between the summer and winter periods. An automatic adjusting solution for PV panels could be technically beneficial; however, it is not advisable from a financial perspective, as the initial investment cost would certainly rise. For the summer season, solution *d* can be considered the preferable one with a total solar incident radiation equal to 2133 kWh, corresponding to a spacing equal to 1.1 m for all orientations and a tilt angle ranging between -55° and -25°. For the winter period, configuration *d* can be the advantageous one with a total incident radiation equal to 761 kWh and 450 m^2 of PV panels.

Regarding the outcomes of the daylight analysis and visual comfort, the research provided valuable insights into the optimal strategies to be implemented to maximize the exploitation of natural lighting to reduce related energy consumption. For industrial facilities with regular shapes and significant surfaces covered, the presence of roof skylights proved to be fundamental to ensure enhanced visual comfort within the working environment, especially in central portions where sunlight coming from side wall windows is insufficient. Similar findings can also be retraced in studies by other authors [28].

Regarding the possible installation of shading systems to avoid or mitigate summer overheating conditions, among the five different filtering solutions, layout (4) proved to be the preferable one, resulting in a decrease in the internal air temperature of about 0.4 °C. Ito et al. [44] affirm that the introduction of a movable solar shading system for south-oriented openings can effectively reduce the cooling demand and produce renewable energy when integrated with PV modules. Their findings demonstrate that the compromise solutions for solar shading systems for south-facing orientation foresee tilt angles ranging from 0° to 10°. Additionally, Nazari et al. [45] suggest that 20° tilted configurations for horizontal slats are the most suitable solutions for south-oriented windows to guarantee acceptable UDI values.

Finally, methodological conclusions can be drawn by comparing the optimization and the design-optioneering methodologies. From the authors' experience, design-optioneering guarantees greater flexibility in analyzing and exploring different design options, especially when no predefined goals are required. However, it may become challenging to implement when dealing with a consistent number of alternatives to be evaluated or with different and conflicting decision criteria. In such cases, optimization procedures may be indicated, as the process is carried out autonomously by the calculation engine, and the interrogation of results through the Pareto front analysis can be more easily handled.

5. Conclusions

In conclusion, the research analyzed some possible retrofit interventions for existing manufacturing buildings. First, the possible integration of PV panels on various facades of the facility was proposed to ensure on-site energy production. Then, the installation of solar shading systems was evaluated for the south-oriented facade to prevent summer overheating within the working space.

For both topics, a multi-objective optimization procedure was applied to a hybrid integration of Grasshopper-based plugins with Design Builder energy simulations.

The most suitable and effective PV panel configuration for different facades was investigated considering both summer and winter solstice conditions. The advisable and

alternative geometrical configurations for solar shading were explored using a design-optioneering approach, considering the summer solstice conditions.

In general, an optimal tilt angle, ranging from $-35°$ to $-75°$, was determined for PV panel installation. Lower tilt angles were preferable for the summer solstice for the south-oriented facade due to the higher solar height. For the summer solstice, the advisable solution for the PV panels was configuration *d*, which features 466 m^2 of PV modules with an incident solar radiation equal to 2133 kWh, effectively balancing the investment costs and system productivity. For the winter solstice, the intermediate tested configurations (*c*, *d*, *e*) provide a total daily incident solar radiation ranging from 632 kWh to 970 kWh. In these cases, the tilt angles tend to be along a vertical direction to maximize the incident solar radiation.

Given the different configurations obtained for winter and summer conditions, an intermediate solution could be advantageous for balancing energy production over the entire year. However, a detailed analysis of the usual seasonal energy demand trends should be carried out. In case of particularly relevant heating or cooling loads for indoor working spaces, configurations that maximize energy production during the winter or summer season should be preferred, respectively. Moreover, the actual availability on the market of the technological components compatible with the selected configuration should be considered. In this regard, the evolution and progress of the currently available elements, which are generally standard or difficult to customize, should be encouraged to meet the developments observed in simulation and analysis tools.

Regarding solar shading systems, the design-optioneering approach provided several alternative solutions to be explored, considering different UDI levels and the amount of solar radiation blocked. Solutions with horizontal (or nearly horizontal) blades are preferable for maximizing the overheating prevention without compromising the availability of natural lighting. The installation of shaders, slightly tilted and 0.4 m spaced on south-oriented windows, results in a decrease in internal air temperature of about 0.5 °C.

In general, the retrofitting measures considered for the representative industrial building analyzed proved to be effective in enhancing energy production and improving the thermal comfort for workers. Moreover, the proposed redevelopment strategies can be applied to the different typological variants of the industrial building type. Other retrofitting solutions could also be tested using similar procedures, encompassing additional evaluation criteria such as the constructability or environmental impact from a life cycle perspective.

From a methodological perspective, the generative design tools used in the research enabled the identification of the most appropriate and valuable solutions through an informed decision-making procedure. The results obtained following similar simulation-based approaches are subject to unavoidable uncertainties related to the input data required. For this reason, validating the outcomes is necessary and recommended. In this study, validation was ensured by comparing the simulated energy demand with the actual data from utility bills provided by the company. However, performing a dedicated sensitivity analysis is advisable to outline the most influential parameters and consequently evaluate whether further assessments are needed.

Author Contributions: Conceptualization, N.B., C.C., F.B. and V.D.N.; methodology, N.B. and C.C.; software, N.B. and C.C.; validation, N.B. and C.C.; data curation, N.B. and C.C.; writing—original draft preparation, N.B. and C.C.; writing—review and editing, N.B., C.C., F.B. and V.D.N.; visualization, N.B. and C.C.; supervision, F.B. and V.DN. All authors have read and agreed to the published version of the manuscript.

Funding: This research received no external funding.

Data Availability Statement: The data presented in this study are available on request from the corresponding author due to ongoing research activities.

Conflicts of Interest: The authors declare no conflicts of interest.

References

1. REN21. REN21.2023 Renewables 2023 Global Status Report Collection, Global Overview. 2023. Available online: https://www.ren21.net/gsr-2023/modules/global_overview/ (accessed on 27 September 2023).
2. United Nations. 2022 Global Status Report for Buildings and Construction. Towards a Zero-Emissions, Efficient and Resilient Buildings and Construction Sector. 2022. Available online: http://globalabc.org/our-work/tracking-progress-global-status-report (accessed on 21 February 2024).
3. European Parliament. P9_TA(2023)0068 Prestazione Energetica Nell'edilizia. Emendamenti del Parlamento Europeo, Approvati il 14 Marzo 2023, alla Proposta di Direttiva del Parlamento Europeo e del Consiglio Sulla Prestazione Energetica Nell'edilizia. 2023. Available online: https://eur-lex.europa.eu/legal-content/IT/ALL/?uri=CELEX:52021PC0558 (accessed on 26 March 2024).
4. European Commission. EU Buiding Stock Observatory. 2017. Available online: https://ec.europa.eu/energy/topics/energy-efficiency/energy-efficient-buildings/eu-bso_en (accessed on 20 January 2023).
5. Banti, N. Existing industrial buildings—A review on multidisciplinary research trends and retrofit solutions. *J. Build. Eng.* **2024**, *84*, 108615. [CrossRef]
6. Minghini, F.; Nerio, T. Seismic Retrofitting Solutions for Precast RC Industrial Buildings Struck by the 2012 Earthquakes in Northern Italy. *Built Environ.* **2021**, *7*, 631315. [CrossRef]
7. Tan, T.; Mills, G.; Papadonikolaki, E.; Liu, Z. Combining multi-criteria decision making (MCDM) methods with building information modelling (BIM): A review. *Autom. Constr.* **2021**, *121*, 103451. [CrossRef]
8. Landim, G.; Digiandomenico, D.; Amaro, J.; Pratschke, A.; Tramontano, M.; Toledo, C. Architectural Optimization and Open Source Development: Nesting and Genetic Algorithms. In Proceedings of the 37th Annual Conference of the Association for Computer Aided Design in Architecture, Cambridge, MA, USA, 2–4 November 2017; pp. 340–349.
9. Holzer, D. Optioneering in Collaborative Design Practic. *J. Archit. Comput.* **2018**, *8*, 165–182.
10. Bazzocchi, F.; Banti, N.; Biagini, C.; Ciacci, C.; Di Naso, V. Design optioneering for the definition of technological solution of the envelope using BIM. In Proceedings of the 17th IBPSA Conference, Bruges, Belgium, 1–3 September 2022; pp. 1451–1458.
11. Eltaweel, A.; Su, Y. Parametric design and daylighting: A literature review. *Renew. Sustain. Energy Rev.* **2017**, *73*, 1086–1103. [CrossRef]
12. Stephan, A.; Prideaux, F.; Crawford, R.H. EPiC grasshopper: A bottom-up parametric tool to quantify life cycle embodied environmental flows of buildings and infrastructure assets. *Build. Environ.* **2024**, *248*, 111077. [CrossRef]
13. Liu, Y.; Li, T.; Xu, W.; Wang, Q.; Huang, H.; He, B.J. Building information modelling-enabled multi-objective optimization for energy consumption parametric analysis in green buildings design using hybrid machine learning algorithms. *Energy Build.* **2023**, *300*, 113665. [CrossRef]
14. Bushra, N. A comprehensive analysis of parametric design approaches for solar integration with buildings: A literature review. *Renew. Sustain. Energy Rev.* **2022**, *168*, 112849. [CrossRef]
15. Zhou, Y. Demand response flexibility with synergies on passive PCM walls, BIPVs, and active air-conditioning system in a subtropical climate. *Renew. Energy* **2022**, *199*, 204–225. [CrossRef]
16. Cicelsky, A.; Meir, I.A. Parametric analysis of environmentally responsive strategies for building envelopes specific for hot hyperarid regions. *Sustain. Cities Soc.* **2014**, *13*, 279–302. [CrossRef]
17. Haghighat, S.; Sadeh, H. Parametric design of an automated kinetic building façade using BIM: A case study perspective. *J. Build. Eng.* **2023**, *73*, 106800. [CrossRef]
18. Salimzadeh, N.; Vahdatikhaki, F.; Hammad, A. Parametric modeling and surface-specific sensitivity analysis of PV module layout on building skin using BIM. *Energy Build.* **2020**, *216*, 109953. [CrossRef]
19. Wong, B.C.L.; Wu, Z.; Gan, V.J.L.; Chan, C.M.; Cheng, J.C.P. Parametric building information modelling and optimality criteria methods for automated multi-objective optimisation of structural and energy efficiency. *J. Build. Eng.* **2023**, *75*, 107068. [CrossRef]
20. Espitia-Mesa, G.; Moreno-Villa, A.; Tobón-Echavarría, S.; Rivera, J.C.; Mejía-Gutiérrez, R. Modeling optimal PV surface of BIPVs for maximum energy yield through Genetic Algorithms. *Energy Built Environ.* 2024, *in press*. [CrossRef]
21. de Sousa Freitas, J.; Cronemberger, J.; Soares, R.M.; Amorim, C.N.D. Modeling and assessing BIPV envelopes using parametric Rhinoceros plugins Grasshopper and Ladybug. *Renew. Energy* **2020**, *160*, 1468–1479. [CrossRef]
22. Fu, Y.; Xu, W.; Wang, Z.; Zhang, S.; Chen, X.; Du, X. Numerical study on comprehensive energy-saving potential of BIPV façade under useful energy utilization for high-rise office buildings in various climatic zones of China. *Sol. Energy* **2024**, *270*, 112387. [CrossRef]
23. Mitsopoulos, G.; Bellos, E.; Tzivanidis, C. Parametric analysis and multi-objective optimization of a solar heating system for various building envelopes. *Therm. Sci. Eng. Prog.* **2018**, *8*, 307–317. [CrossRef]
24. Qingsong, M.; Fukuda, H. Parametric Office Building for Daylight and Energy Analysis in the Early Design Stages. *Procedia—Soc. Behav. Sci.* **2016**, *216*, 818–828. [CrossRef]
25. Alsharif, R.; Arashpour, M.; Golafshani, E.; Rashidi, A.; Li, H. Multi-objective optimization of shading devices using ensemble machine learning and orthogonal design of experiments. *Energy Build.* **2023**, *283*, 112840. [CrossRef]
26. Li, L.; Ma, Q.; Gao, W.; Wei, X. Incorporating users' adaptive behaviors into multi-objective optimization of shading devices: A case study of an office room in Qingdao. *Energy Build.* **2023**, *301*, 113683. [CrossRef]

27. Reisinger, J.; Zahlbruckner, M.A.; Kovacic, I.; Kán, P.; Wang-Sukalia, X.; Kaufmann, H. Integrated multi-objective evolutionary optimization of production layout scenarios for parametric structural design of flexible industrial buildings. *J. Build. Eng.* **2022**, *46*, 103766. [CrossRef]
28. Dolnikova, E.; Dolnik, B. Comparison of different roof types in terms of lighting conditions in an industrial hall. *Adv. Civ. Archit. Eng.* **2022**, *24*, 23–31. [CrossRef]
29. Mavridou, T.; Doulos, L.T. Evaluation of Different Roof Types Concerning Daylight in Industrial Buildings during the Initial Design Phase: Methodology and Case Study. *Buildings* **2019**, *9*, 170. [CrossRef]
30. Lin, Q.; Kensek, K.; Schiler, M.; Choi, J. Streamlining sustainable design in building information modeling BIM-based PV design and analysis tools. *Archit. Sci. Rev.* **2021**, *64*, 467–477. [CrossRef]
31. Octopus Plugin for Grasshopper. Available online: https://www.food4rhino.com/en/app/octopus (accessed on 17 October 2023).
32. Honeybee Plugin for Grasshopper. Available online: https://www.ladybug.tools/honeybee.html (accessed on 17 October 2023).
33. *UNI EN ISO 12464-1*; Illuminazione dei Posti di Lavoro. Ente Nazionale di Normazione: Rome, Italy, 2004.
34. Colibri Plugin for Grasshopper. Available online: http://core.thorntontomasetti.com/colibri-release/ (accessed on 17 October 2023).
35. DesignExplorer. Available online: https://www.thorntontomasetti.com/capability/design-explorer (accessed on 13 December 2023).
36. Governo italiano. *Regolamento Recante Norme per la Progettazione, l'installazione, l'esercizio e la Manutenzione degli Impianti Termici degli Edifici ai fini del Contenimento dei Consumi di Energia, in Attuazione dell'art. 4, Comma 4, della legge 9 Gennaio 1991, n. 10*; Governo Italiano: Rome, Italy, 1993.
37. Nabil, A.; Mardaljevic, J. Useful daylight illuminances: A replacement for daylight factors. *Energy Build.* **2006**, *38*, 905–913. [CrossRef]
38. Katunský, D.; Dolníková, E.; Doroudiani, S. Integrated lighting efficiency analysis in large industrial buildings to enhance indoor environmental quality. *Buildings* **2017**, *7*, 47. [CrossRef]
39. Martín-Chivelet, N.; Gutiérrez, J.C.; Alonso-Abella, M.; Chenlo, F.; Cuenca, J. Building Retrofit with Photovoltaics: Construction and Performance of a BIPV Ventilated Façade. *Energies* **2018**, *11*, 1719. [CrossRef]
40. Reffat, R.M.; Ezzat, R. Impacts of design configurations and movements of PV attached to building facades on increasing generated renewable energy. *Sol. Energy* **2023**, *252*, 50–71. [CrossRef]
41. Paydar, M.A. Optimum design of building integrated PV module as a movable shading device. *Sustain. Cities Soc.* **2020**, *62*, 102368. [CrossRef]
42. Nicoletti, F.; Cucumo, M.A.; Arcuri, N. Building-integrated photovoltaics (BIPV): A mathematical approach to evaluate the electrical production of solar PV blinds. *Energy* **2023**, *263*, 126030. [CrossRef]
43. Menichini, G.; Del Monte, E.; Orlando, M.; Vignoli, A. *Out-of-Plane Capacity of Cladding Panel-to-Structure Connections in One-Story R/C Precast Structures*; Springer: Dordrecht, The Netherlands, 2020; Volume 18.
44. Ito, R.; Lee, S. Development of adjustable solar photovoltaic system for integration with solar shading louvers on building façades. *Appl. Energy* **2024**, *359*, 122711. [CrossRef]
45. Nazari, S.; MirzaMohammadi, P.K.; Sajadi, B.; Ha, P.P.; Talatahari, S.; Sareh, P. Designing energy-efficient and visually-thermally comfortable shading systems for office buildings in a cooling-dominant climate. *Energy Rep.* **2023**, *10*, 3863–3881. [CrossRef]